Acta Polytechnica **64**(4):297–313, 2024
https://doi.org/10.14311/AP.2024.64.0297

NON-HOMOGENEITY EFFECT ON THE VIBRATION OF THE RECTANGULAR VISCO-ELASTIC PLATE SUBJECTED TO THE LINEAR TEMPERATURE EFFECT WITH QUADRATIC THICKNESS VARIATION IN BOTH DIRECTIONS

Sudhanshu Aggarwal

National Post Graduate College Barhalganj, Department of Mathematics, Gorakhpur-273402, Uttar Pradesh, India

correspondence: sudhanshu30187@gmail.com

Abstract. The present work investigates the effect of non-homogeneity on the vibration of a rectangular visco-elastic plate. The plate is subjected to linear temperature variation in the x-direction with quadratic thickness variation in both directions. The quadratic variation has been considered in the material density of the plate only along the x-axis, and it is assumed that non-homogeneity transpires because of this variation. The governing differential equation is solved using the Rayleigh-Ritz technique. All four edges of the plate should be clamped to drive the frequency equation. Deflection and time period have been evaluated for several combinations of values of the thermal constant, constant of nonhomogeneity, taper constants, and length-to-width ratio (aspect ratio) for the first two vibration modes of the clamped plate. The results presented are compared with those found in the literature.

Keywords: Rayleigh-Ritz technique, taper constants, clamped plate, differential equation, thermal constant.

1. Introduction

Due to their practical and scholarly interests, the vibration problems of elasticity have been the subject of effort or research for a considerable amount of time. Machines often produce heat as a result of vibration, which reduces machine efficiency. As a result, it is critical to investigate variations in temperature on vibration-affected plates.

There are a number of materials, found in nature that are nonhomogeneous (e.g. delta wood, plywood, timber, fibre reinforced plastics, etc.). The use of these natural nonhomogeneous materials in the industry is generally due to their nature to strengthen the construction. Glass epoxy and boron epoxy in the steel alloys are examples of the artificial nonhomogeneous materials used in the manufacture of nuclear reactor rods. The non-homogeneity in the materials arises due to imperfections in the material, them being composite materials, or work under elevated temperatures [1]. Sharma and Sarkar [2, 3] suggested another common way to introduce the non-homogeneity in the plate by attaching a mass, spring, or a spring-mass system to it. Today, scientists and engineers are developing new materials to meet the demands of high temperatures and high strength services. Duralium (Alloy of Aluminium, Copper, Magnesium and Manganese) is the material that is widely used in the defence industry (aircraft fittings, space booster tank age, forgings, pistons of aircraft engine, compressor rings, and impellers of the jet engine) due to its very attractive idiosyncrasy like the high strength, and the light weight. Duralium material parameters are used for the numerical computation in this study.

In concrete, most of the materials used in industrial applications become visco-elastic due to the very high temperature rise and these materials deviate from the Hooke's law of elasticity, which states that within the elastic limits, the stress is directly proportional to the strain. The behaviour (elastic or viscous) of the material depends on the two parameters, the temperature and the frequency (the rate of the loading). Ceramics (rocks, concrete, inorganic glassy materials, piezoelectric ceramics), biological composite materials (wood, plant seeds, tissue), and many polymers (plastic, rubber, vinyl, acrylics, silicones, adhesive, etc.) are the generally used visco-elastic materials.

Although the uniform thickness plates are commonly used, the use of variable thickness plates is also common, such as rocket fins, the wing panels in the aerospace engineering, disc wheels and car body panels in mechanical engineering, building walls, and floors in civil engineering, off-shore platforms, and ship decks in marine engineering, and printed circuit boards in electronics, in example. Plates of the variable thickness have the wide practice in many fields of the engineering due to the some very attractive idiosyncrasy of their like the high strength, and the stiffness, the reduction of the cost, and the minimizing the size, and the weight.

Gupta and Kumar [4] used the Galerkin's technique and analysed the vibration of a non-homogeneous visco-elastic plate (rectangular) in the thermal environment with the linear variation of the thickness. Gupta and Khanna [5, 6] studied the vibration of the variable thickness rectangular visco-elastic plate using the Rayleigh-Ritz technique. Gupta et al. [7] determined the fundamental frequencies and the deflection by analysing the vibration of the non-homogeneous orthotropic plate (rectangular) having linear thickness variations in both the directions with the thermal gradient effect. Gupta and Kaur [8] used the Rayleigh-Ritz method to determine the thermal gradient effect on the vibration of the variable thickness visco-elastic rectangular plate with clamped boundary conditions. The monograph of Leissa [1] has an excellent literature on the vibration of the plates for the scholars and it is very convenient to curb the duplication of the research handiwork in the plate vibrations.

Singh and Saxena [9] have determined the vibration (transverse) of the rectangular plate and they have considered the bidirectional thickness variation in this study. Laura and Gutierrez [10] analysed the vibration of the rectangular plate with the thermal gradient effect. Gupta et al. [11] considered the Rayleigh-Ritz technique for analysing the vibrations of the variable thickness rectangular visco-elastic plate. Gupta and Aggarwal [12–14] discussed the linear temperature effect on the vibration of a non-homogeneous visco-elastic plate (rectangular) with variable thickness in two directions. Gupta and Kaur [15] have considered the linear temperature variation and studied its effect on the free transverse vibration of the clamped visco-elastic rectangular plate exponential thickness variation in both directions. Nagaya [16] found solutions to the problems of vibration and transient response of the non-periodic elastically supported continuous visco-elastic plates. Gupta et al. [17] analysed the thermal effect on the vibration problem of the clamped visco-elastic rectangular plate. Bhat [18] determined the natural frequencies of the rectangular plates using the Rayleigh-Ritz method.

Tomar and Gupta [19] studied the vibration problem of an orthotropic rectangular plate with the linearly varying thickness and determined the thermal effect on the frequencies of the plate considered. Saini and Lal [20] used the general differential quadrature (GDQ) method to analyse the transverse vibration of the variable thickness non-homogeneous rectangular plates. Gupta et al. [21] considered the linearly varying thickness non-homogeneous rectangular plate and analysed its vibration. Sobamowo et al. [22] applied the three-dimensional differential transformation method to the problem of thermally induced vibration of the non-homogeneous rectangular plate with the varying thickness. Shabnam et al. [23] studied the problem of free vibration of thin plates with the variable thickness and determined its solution using the two-dimensional differential transformation method. Singhal and Ruby [24] discussed the thermally induced vibrations of the tapered non-homogeneous rectangular plate. Yeh et al. [25] used the finite difference, and the differential transformation methods to determine the solution to the free vibration problem of the plate.

Khanna and Singhal [26] studied the vibration problem of a clamped visco-elastic thin plate (rectangular). Jafari and Azhari [27] discussed the problem of free vibration of visco-elastic plate (Mindlin) and determined the natural frequency along with viscous damping. Amabili et al. [28] obtained the solutions of the problems of nonlinear vibration of fractional visco-elastic rectangular plates with damping. Bhardwaz et al. [29] determined the time period for the vibration problem of a non-homogeneous parallelogram plate (skew) with two-dimensional parabolic temperature variations. Abdikarimov et al. [30] discussed the problem of dynamic stability of a orthotropic visco-elastic plate (rectangular) with arbitrary thickness variation.

This work aims to analyse the non-homogeneity effect of vibrations on the rectangular visco-elastic plate subjected to a linear temperature effect with quadratic thickness variation in both directions. The deflection (w) and time period (t_p) have been evaluated for several combinations of the values of the thermal constant (α), constant of the non-homogeneity (α_1), taper constants (β_1, β_2) and the length-to-width ratio ($\frac{a}{b}$) for the first two vibration modes of a clamped plate. Graphs and tables are used for presenting the corresponding results. The rest of this paper is organised as follows. Assumptions of the study are provided in Section 2. Equation of the motion and the method of the analysis are presented in Section 3. We present differential equation of the time function with its solution in Section 4. All the results and discussions are presented in Section 5. The comparison of the results of the present study with the previous study is provided in Section 6. The last section (Section 7) presents a brief conclusion.

2. Assumptions of the study

Author has considered the following assumptions for this study:

- The quadratic variation has been considered in the material density of the plate only along the x-axis. In addition, it is supposed that the non-homogeneity occurs due to this variation.
- It is supposed that all the four edges of the plate are clamped for deriving the frequency equation with the use of the Rayleigh-Ritz technique. According to this technique, the maximum strain energy must be equal to the maximum kinetic energy.
- The linear variation in the temperature of the plate has been considered only along the x-axis.
- The quadratic variation has been considered for the thickness of the plate along the x-axis and the y-axis.
- The linear visco-elastic behaviour is of the Kelvin type.
- The assumption of the small deflection is assumed.
- Duralium material (Alloy of Aluminium, Copper, Magnesium, and Manganese) parameters are used for the numerical computation.

3. Equation of the motion and the method of the analysis

The author discusses the equation of the motion and the method of the analysis in this section.

For the free vibration of the plate, the transverse motion and the time function are given by the following equations, respectively, as [15]:

$$\left[\left\{\begin{array}{l} D\left(\frac{\partial^4 W}{\partial x^4}+2\frac{\partial^4 W}{\partial x^2\partial y^2}+\frac{\partial^4 W}{\partial y^4}\right) \\ +2\frac{\partial D}{\partial x}\left(\frac{\partial^3 W}{\partial x^3}+\frac{\partial^3 W}{\partial x\partial y^2}\right) \\ +2\frac{\partial D}{\partial y}\left(\frac{\partial^3 W}{\partial y^3}+\frac{\partial^3 W}{\partial x^2\partial y}\right) \\ +\frac{\partial^2 D}{\partial x^2}\left(\frac{\partial^2 W}{\partial x^2}+\nu\frac{\partial^2 W}{\partial y^2}\right) \\ +\frac{\partial^2 D}{\partial y^2}\left(\frac{\partial^2 W}{\partial y^2}+\nu\frac{\partial^2 W}{\partial x^2}\right) \\ +2\left(1-\nu\right)\frac{\partial^2 D}{\partial x\partial y}\frac{\partial^2 W}{\partial x\partial y} \end{array}\right\}-\rho h k^2 W=0\right], \quad (1)$$

and:

$$\ddot{T}+k^2\widetilde{D}T=0, \quad (2)$$

where:

$$D=\frac{Eh^3}{12\left(1-\nu^2\right)}, \quad (3)$$

is the flexural rigidity,

ν is the Poisson's ratio,

E is the Young modulus of elasticity,

ρ is the density,

h is the thickness of the plate,

$\widetilde{D}$ is the unique Rheological operator,

k is the frequency,

T is the time function,

W is the deflection function,

$\ddot{T}$ is the second derivative of the time function with respect to time t.

Let's consider a symmetrical plate (rectangular) with all four edges clamped at length a and width b, see Figure 1.

Assuming that the plate under consideration has the linear temperature variation only along the x-axis:

$$\tau=\tau_0\left(1-\frac{x}{a}\right), \quad (4)$$

where τ_0 and τ denote the temperature increment above the reference temperature at any point at the end $x=a$ and at the distance $\left(\frac{x}{a}\right)$, respectively.

The modulus of the elasticity (temperature dependent) can be expressed as [16]:

$$E=E_0\left(1-\gamma\tau\right), \quad (5)$$

where

E_0 is the modulus of elasticity at $\tau=0$ (reference temperature),

γ is the slope of the variation of E with τ.

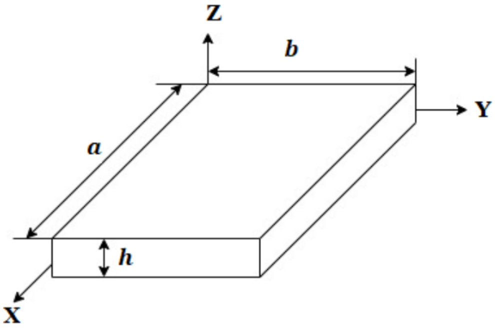

Figure 1. Rectangular plate with length a and width b.

Substituting the Equation (4) into the Equation (5) provides:

$$E=E_0\left[1-\alpha\left(1-\frac{x}{a}\right)\right], \quad (6)$$

where the parameter $\alpha=\gamma\tau_0$ is called the thermal gradient and has a value in the interval $[0,1]$. Suppose that the plate under consideration has a quadratic thickness variation in both directions:

$$h=h_0\left(1+\beta_1\frac{x^2}{a^2}\right)\left(1+\beta_2\frac{y^2}{b^2}\right), \quad (7)$$

where

β_1 is the taper constant along the x-axis,

β_2 is the taper constant along the y-axis,

h_0 is the thickness of the plate at $x=y=0$.

Assuming that the density ρ of the plate under consideration has the parabolic variation along the x-axis, given by:

$$\rho=\rho_0\left(1+\alpha_1\frac{x^2}{a^2}\right), \quad (8)$$

where

α_1 is the non-homogeneity constant,

ρ_0 is the value of the density at $x=0$.

The deflection function (w) can be considered in the following form for the free vibrations (transverse) of the plate [12]:

$$w(x,y,t)=T(t)\,W(x,y). \quad (9)$$

Leissa [1] defined the strain energy S and the kinetic energy P as:

$$S=\frac{1}{2}\int_0^a\int_0^b D\left[\left(\frac{\partial^2 W}{\partial y^2}\right)^2+\left(\frac{\partial^2 W}{\partial x^2}\right)^2+2\left(1-\nu\right)\left(\frac{\partial^2 W}{\partial x\partial y}\right)^2+2\nu\frac{\partial^2 W}{\partial x^2}\frac{\partial^2 W}{\partial y^2}\right]dxdy, \quad (10)$$

and

$$P=\frac{1}{2}k^2\int_0^a\int_0^b \rho h W^2 dxdy. \quad (11)$$

The expression of the flexural rigidity using the Equations (6) and (7) (assuming ν is the constant) in the Equation (3) can be written as:

$$D = \frac{1}{12\left(1-\nu^2\right)}\left[E_0 {h_0}^3\left\{1-\alpha\left(1-\frac{x}{a}\right)\right\}\left(1+\beta_1\frac{x^2}{a^2}\right)^3\left(1+\beta_2\frac{y^2}{b^2}\right)^3\right]. \tag{12}$$

Substituting Equations (7) and (8) into the Equation (11) gives:

$$P = \frac{1}{2}\rho_0 h_0 k^2 \int_0^a \int_0^b \left(1+\alpha_1\frac{x^2}{a^2}\right)\left(1+\beta_1\frac{x^2}{a^2}\right)\left(1+\beta_2\frac{y^2}{b^2}\right) W^2 dx dy. \tag{13}$$

The principle of the Rayleigh-Ritz technique [14] provides:

$$\delta(S-P)=0, \tag{14}$$

The assumption that the four edges of the rectangular plate are clamped gives:

$$\begin{cases}(W)_{x=0} = (W)_{x=a} = \left(\frac{\partial W}{\partial x}\right)_{x=0} = \left(\frac{\partial W}{\partial x}\right)_{x=a} = 0,\\ (W)_{y=0} = (W)_{y=b} = \left(\frac{\partial W}{\partial y}\right)_{y=0} = \left(\frac{\partial W}{\partial y}\right)_{y=b} = 0.\end{cases} \tag{15}$$

Taking the deflection function $W(x,y)$ as [13]:

$$W(x,y) = \left\{\left[\left(\frac{y}{b}\right)\left(\frac{x}{a}\right)\left(1-\frac{y}{b}\right)\left(1-\frac{x}{a}\right)\right]^2 \left[L_1 + L_2\left(\frac{y}{b}\right)\left(\frac{x}{a}\right)\left(1-\frac{y}{b}\right)\left(1-\frac{x}{a}\right)\right]\right\}, \tag{16}$$

where both constants L_1 and L_2 are satisfied by the Equation (15).

Now, taking the non-dimensional quantities in the capital letters as [13]:

$$\begin{cases}\bar{h} = \left(\frac{h}{a}\right),\\ \bar{W} = \left(\frac{W}{a}\right),\\ X = \left(\frac{x}{a}\right),\\ Y = \left(\frac{y}{a}\right).\end{cases} \tag{17}$$

Using Equation (17) in Equation (16) gives:

$$W = \left[Y\left(\frac{a}{b}\right)X\left(1-Y\left(\frac{a}{b}\right)\right)(1-Y)\right]^2 \left[L_1 + L_2 Y\left(\frac{a}{b}\right)X\left(1-Y\left(\frac{a}{b}\right)\right)(1-X)\right]. \tag{18}$$

Using Equations (12), and (17) in Equations (10) and (13) gives:

$$S = C\int_0^1\int_0^{\frac{b}{a}}\left[\left[\{1-\alpha(1-X)\}\left(1+\beta_1 X^2\right)^3\left(1+\beta_2 Y^2\frac{a^2}{b^2}\right)^3\right]\left[\left(\frac{\partial^2\bar{W}}{\partial Y^2}\right)^2 + \left(\frac{\partial^2\bar{W}}{\partial X^2}\right)^2 + 2(1-\nu)\left(\frac{\partial^2\bar{W}}{\partial X\partial Y}\right)^2 + 2\nu\frac{\partial^2\bar{W}}{\partial X^2}\frac{\partial^2\bar{W}}{\partial Y^2}\right]\right] dX dY, \tag{19}$$

where $C = \frac{E_0 \bar{h_0}^3 a^3}{24(1-\nu^2)}$ and:

$$P = \frac{1}{2}\rho_0 \bar{h_0} k^2 a^5 \int_0^1\int_0^{\frac{b}{a}}\left(1+\alpha_1 X^2\right)\left(1+\beta_1 X^2\right)\left(1+\beta_2 Y^2\frac{a^2}{b^2}\right)\bar{W}^2 dX dY. \tag{20}$$

Using Equations (19) and (3) in Equation (14) gives:

$$\delta\left(S_1 - n^2 k^2 P_1\right) = 0, \tag{21}$$

where:

$$S_1 = \int_0^1\int_0^{b/a}\left[\left[\{1-\alpha(1-X)\}\left(1+\beta_1 X^2\right)^3\left(1+\beta_2 Y^2\frac{a^2}{b^2}\right)^3\right]\left[\left(\frac{\partial^2\bar{W}}{\partial Y^2}\right)^2 + \left(\frac{\partial^2\bar{W}}{\partial X^2}\right)^2 + 2(1-\nu)\left(\frac{\partial^2\bar{W}}{\partial X\partial Y}\right)^2 + 2\nu\frac{\partial^2\bar{W}}{\partial X^2}\frac{\partial^2\bar{W}}{\partial Y^2}\right]\right] dX dY, \tag{22}$$

and:

$$P_1 = \int_0^1\int_0^{b/a}\left(1+\alpha_1 X^2\right)\left(1+\beta_1 X^2\right)\left(1+\beta_2 Y^2\frac{a^2}{b^2}\right)\bar{W}^2 dX dY. \tag{23}$$

Here:

$$n^2 = \left\{\frac{12\rho_0\left(1-\nu^2\right)a^2}{E_0 \bar{h_0}^2}\right\}. \tag{24}$$

The two unknown parameters L_1 and L_2 that are appearing by substituting W from Equation (16) into equation (21) can be computed as:

$$\begin{cases}\frac{\partial}{\partial B_1}(S_1 - n^2k^2P_1) = 0,\\ \text{and } \frac{\partial}{\partial B_2}(S_1 - n^2k^2P_1) = 0.\end{cases} \tag{25}$$

Solution of Equation (25) provides:

$$\begin{cases}d_{11}L_1 + d_{12}L_2 = 0,\\ d_{21}L_1 + d_{22}L_2 = 0,\end{cases} \tag{26}$$

S.N.	Parameters	Values
1.	Young modulus of the elasticity ($\mathrm{N\,m^{-2}}$), E	7.08×10^{10}
2.	Shear modulus ($\mathrm{N\,m^{-2}}$), G	2.682×10^{10}
3.	Visco-elastic constant ($\mathrm{Ns\,m^{-2}}$), η	1.4612×10^{6}
4.	Density ($\mathrm{kg\,m^{-3}}$), ρ	2.80×10^{3}
5.	Poisson's ratio, ν	0.345

TABLE 1. Duralium material (Alloy of Aluminum, Copper, Magnesium, and Manganese) parameters that are used for the numerical computation [16].

where d_{11}, d_{12}, d_{21}, d_{22} involve the frequency parameter and the parametric constants.

The non-trivial solution of the Equation (26) is obtained by:

$$\begin{vmatrix} d_{11} & d_{12} \\ d_{21} & d_{22} \end{vmatrix} = 0. \tag{27}$$

Equation (27) is a quadratic equation in k^2 and it is known as the frequency equation. Solving Equation (27) gives the two values of k^2.

Now, if we choose $L_1 = 1$ and substitute it into Equation (26), we have $L_2 = -\left(\frac{d_{11}}{d_{12}}\right)$.

Using the above values for L_1, and L_2 in Equation (18) suggests that:

$$\begin{aligned} W = &\left[Y\left(\frac{a}{b}\right)X\left(1-Y\left(\frac{a}{b}\right)\right)(1-X)\right]^2 \\ &\left[1+\left(-\frac{d_{11}}{d_{12}}\right)Y\left(\frac{a}{b}\right)X\left(1-Y\left(\frac{a}{b}\right)\right)(1-X)\right]. \end{aligned} \tag{28}$$

4. Differential equation of the time function with its solution

The author has derived the differential equation of the time function and then he has given its solution in this section.

The unique rheological operator $\widetilde{D}$ for the consideration of linear visco-elastic model (model of the Kelvin) is given as [13]:

$$\widetilde{D} \equiv \left[1 + \left(\frac{\eta}{G}\right)\left(\frac{d}{dt}\right)\right], \tag{29}$$

where

η is visco-elastic constant,

G is shear modulus.

Using Equation (29) in Equation (2) gives:

$$\ddot{T} + k^2\left(\frac{\eta}{G}\right)\dot{T} + k^2 T = 0. \tag{30}$$

The solution of the Equation (30) will be of the form:

$$T(t) = e^{a_1 t}(A\cos b_1 t + B\sin b_1 t), \tag{31}$$

where:

$$\begin{cases} a_1 = -\dfrac{k^2}{2}\left(\dfrac{\eta}{G}\right), \\ b_1 = k\sqrt{1-\left(\dfrac{\rho\eta}{2G}\right)^2}, \\ A,\ B = \text{constants}. \end{cases} \tag{32}$$

Consider the following initial conditions for determining the values of A and B:

$$\text{At } t = 0, T = 1 \text{ and } \dot{T} = 0. \tag{33}$$

Using Equation (33) in Equation (31) provides:

$$\begin{cases} A = 1, \\ B = -\dfrac{a_1}{b_1}. \end{cases} \tag{34}$$

After substituting the values of A, B into Equation (31), one obtains:

$$T(t) = e^{a_1 t}\left(\cos b_1 t - \frac{a_1}{b_1}\sin b_1 t\right). \tag{35}$$

Thus, $w(x, y, t)$ can be expressed using Equations (28) and (35) in Equation (9) as:

$$\begin{aligned} w = &\left\{Y\left(\frac{a}{b}\right)X\left(1-Y\left(\frac{a}{b}\right)\right)(1-X)\right\}^2 \\ &\left\{1-\left(\frac{b_{11}}{b_{12}}\right)Y\left(\frac{a}{b}\right)X\left(1-Y\left(\frac{a}{b}\right)\right)(1-X)\right\} \\ &\left\{e^{a_1 t}\left(cosb_1 t - \left(\frac{a_1}{b_1}\right)sinb_1 t\right)\right\}. \end{aligned} \tag{36}$$

For the vibration of the plate, the relation of the time period (t_p) with the frequency (k) is expressed by [13]:

$$t_p = \frac{2\pi}{k}, \tag{37}$$

where the frequency k is easily determined using Equation (27).

5. Results and discussions

In the present work, the time period (t_p) and the deflection (w) are determined for various combinations of the values of (α), $\left(\frac{a}{b}\right)$, (β_1, β_2), and (α_1) for the first two modes of vibration and are given in Tables 2–12. The quadratic variation has been considered in the material density of the plate only along the x-axis. In the calculation, the thickness at the centre of the rectangular plate was taken as 0.01 m. The material (Duralium) parameters used for the computational work are presented in Table 1.

Table 2 deals with the variation of t_p (*10^{-6} in seconds) with different values of α (0.0, 0.2, 0.4, 0.6, 0.8, 1.0), and constant $\frac{a}{b} = 1.5$ for all X and Y. The continuous increments are observed in the values of

Mode →	$\alpha_1 = 0.0$				$\alpha_1 = 0.4$			
	$\beta_1 = 0.0$, $\beta_2 = 0.0$		$\beta_1 = 0.4$, $\beta_2 = 0.2$		$\beta_1 = 0.0$, $\beta_2 = 0.0$		$\beta_1 = 0.4$, $\beta_2 = 0.2$	
α ↓	I	II	I	II	I	II	I	II
0.0	6 462	1 623	5 324	1 332	6 897	1 728	5 543	1 433
0.2	6 823	1 731	5 513	1 438	7 246	1 856	5 849	1 496
0.4	7 236	1 863	5 874	1 497	7 733	2 002	6 194	1 617
0.6	7 737	2 002	6 213	1 603	8 497	2 176	6 626	1 759
0.8	8 443	2 168	6 584	1 737	9 220	2 285	7 082	1 846
1.0	9 231	2 304	7 117	1 863	9 668	2 439	7 530	1 988

Table 2. Variation of t_p (*10^{-6} in seconds) with different α and constant $\frac{a}{b} = 1.5$ for all X and Y see Figure 2.

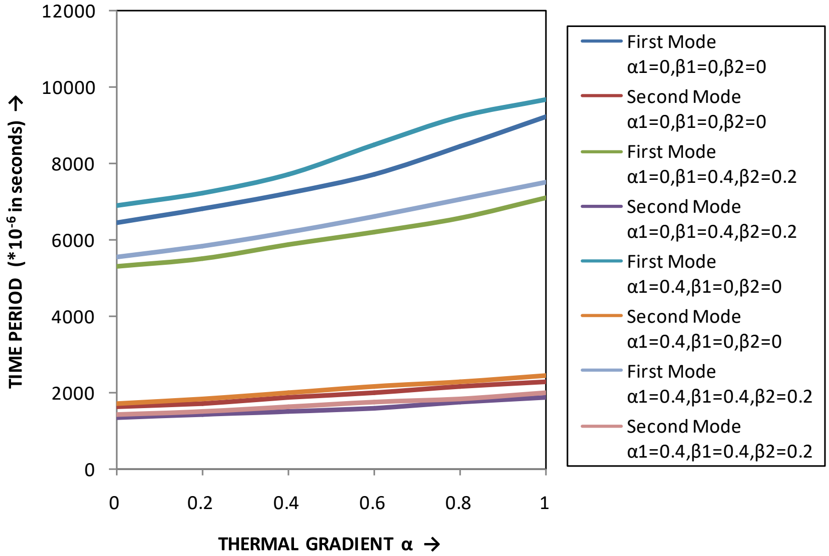

Figure 2. Variation of t_p (*10^{-6} in seconds) with different α and constant $\frac{a}{b} = 1.5$ for all X and Y.

Mode →	$\alpha_1 = 0.0$				$\alpha_1 = 0.4$			
	$\beta_1 = 0.0$, $\beta_2 = 0.0$, $\alpha = 0.0$		$\beta_1 = 0.4$, $\beta_2 = 0.2$, $\alpha = 0.3$		$\beta_1 = 0.0$, $\beta_2 = 0.0$, $\alpha = 0.0$		$\beta_1 = 0.4$, $\beta_2 = 0.2$, $\alpha = 0.3$	
$\frac{a}{b}$ ↓	I	II	I	II	I	II	I	II
0.5	15 559	3 878	13 873	3 417	16 023	4 008	14 296	3 557
1.0	10 411	2 638	9 657	2 471	10 860	2 747	9 971	2 588
1.5	6 462	1 623	5 697	1 465	6 897	1 728	6 021	1 515
2.0	3 724	905	3 513	873	4 082	961	3 864	957
2.5	2 451	576	2 391	560	2 771	658	2 739	651

Table 3. Variation of t_p (*10^{-6} in seconds) with different $\frac{a}{b}$ for all X and Y, see Figure 3.

t_p as α increases from 0.0 to 1.0 for both modes of vibration. The graph shown in Figure 2 supports the results of Table 2.

Table 3 is concerned with the variation of t_p (*10^{-6} in seconds) with different $\frac{a}{b}$(0.5, 1.0, 1.5, 2.0, 2.5) for all X and Y. The continuous decrements are observed in the values of t_p as $\frac{a}{b}$ increases from 0.5 to 2.5 for modes of vibration. The results of Table 3 are supported by the graph shown in Figure 3.

Table 4 shows the variation of t_p (*10^{-6} in seconds) with different β_1(0.0, 0.2, 0.4, 0.6, 0.8, 1.0) and constant $\frac{a}{b} = 1.5$ for all X and Y. It is observed that as the value of β_1 increases from 0.0 to 1.0, the value of t_p decreases for both modes of vibration. The graph in Figure 4 supports the results of Table 4.

Table 5 shows the variation of t_p (*10^{-6} in seconds) with different β_2(0.0, 0.2, 0.4, 0.6, 0.8, 1.0) and constant $\frac{a}{b} = 1.5$ for all X and Y. From this table, it can clearly be seen that the value of t_p decreases as β_2 increases from 0.0 to 1.0 for both the vibration

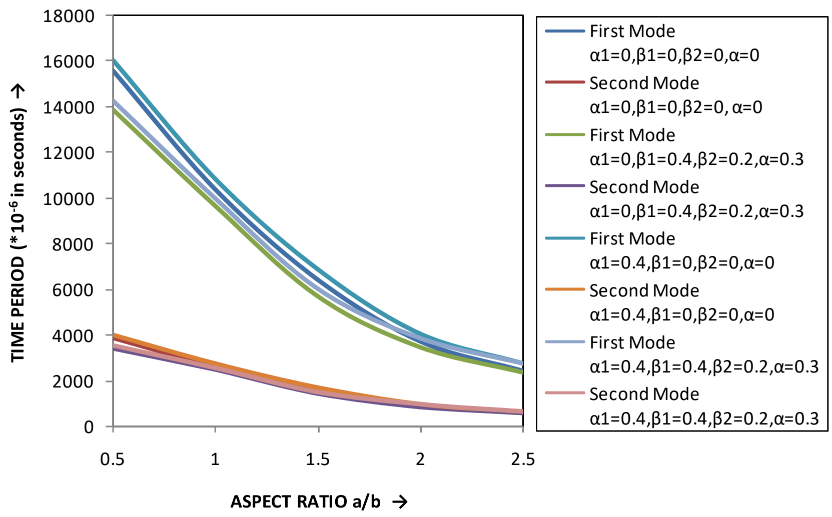

Figure 3. Variation of t_p (*10^{-6} in seconds) with different $\frac{a}{b}$ for all X and Y.

	$\alpha_1 = 0.0$				$\alpha_1 = 0.4$			
	$\beta_2 = 0.0$, $\alpha = 0.0$		$\beta_2 = 0.2$, $\alpha = 0.3$		$\beta_2 = 0.0$, $\alpha = 0.0$		$\beta_2 = 0.2$, $\alpha = 0.3$	
Mode → / β_1 **↓**	**I**	**II**	**I**	**II**	**I**	**II**	**I**	**II**
0.0	6 462	1 623	6 360	1 564	6 897	1 728	6 702	1 701
0.2	6 123	1 566	6 011	1 503	6 543	1 618	6 336	1 600
0.4	5 784	1 489	5 697	1 465	6 216	1 568	6 021	1 515
0.6	5 402	1 373	5 278	1 327	5 930	1 453	5 591	1 437
0.8	5 087	1 285	4 923	1 213	5 433	1 365	5 242	1 343
1.0	4 736	1 207	4 642	1 128	5 141	1 297	4 971	1 260

Table 4. Variation of t_p (*10^{-6} in seconds) with different β_1 and constant $\frac{a}{b} = 1.5$ for all X and Y, see Figure 4.

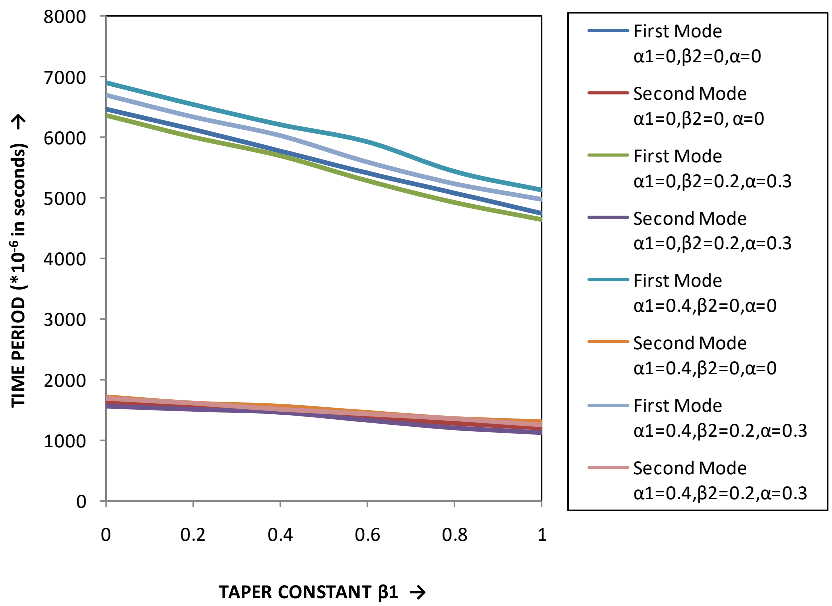

Figure 4. Variation of t_p (*10^{-6} in seconds) with different β_1 and constant $\frac{a}{b} = 1.5$ for all X and Y.

	$\alpha_1 = 0.0$				$\alpha_1 = 0.4$			
	$\beta_1 = 0.0$		$\beta_1 = 0.4$		$\beta_1 = 0.0$		$\beta_1 = 0.4$	
	$\alpha = 0.0$		$\alpha = 0.3$		$\alpha = 0.0$		$\alpha = 0.3$	
Mode $\rightarrow$ $\beta_2 \downarrow$	**I**	**II**	**I**	**II**	**I**	**II**	**I**	**II**
0.0	6 462	1 623	6 033	1 512	6 897	1 728	6 504	1 681
0.2	6 102	1 543	5 697	1 465	6 537	1 609	6 021	1 515
0.4	5 761	1 462	5 318	1 324	6 193	1 537	5 576	1 446
0.6	5 384	1 356	4 866	1 243	5 903	1 429	5 167	1 333
0.8	5 049	1 253	4 613	1 117	5 413	1 316	4 791	1 211
1.0	4 703	1 184	4 264	1 058	4 998	1 251	4 448	1 135

Table 5. Variation of t_p (*10^{-6} in seconds) with different β_2 and constant $\frac{a}{b} = 1.5$ for all X and Y, see Figure 5.

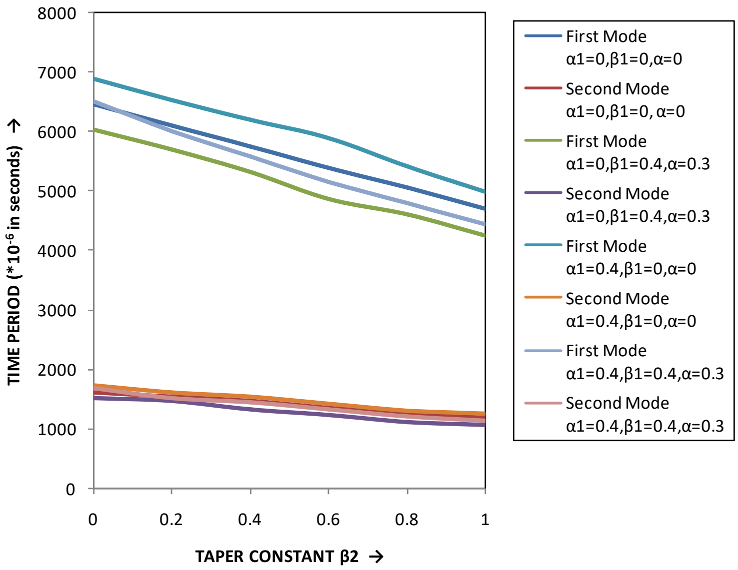

Figure 5. Variation of t_p (*10^{-6} in seconds) with different β_2 and constant $\frac{a}{b} = 1.5$ for all X and Y.

	$\alpha = 0.0$				$\alpha = 0.3$			
	$\beta_1 = 0.0$		$\beta_1 = 0.4$		$\beta_1 = 0.0$		$\beta_1 = 0.4$	
	$\beta_2 = 0.0$		$\beta_2 = 0.2$		$\beta_2 = 0.0$		$\beta_2 = 0.2$	
Mode $\rightarrow$ $\alpha_1 \downarrow$	**I**	**II**	**I**	**II**	**I**	**II**	**I**	**II**
0.0	6 462	1 623	5 324	1 332	7 083	1 833	5 697	1 465
0.2	6 695	1 687	5 511	1 426	7 291	1 890	5 889	1 504
0.4	6 897	1 728	5 543	1 433	7 489	1 930	6 021	1 515
0.6	7 096	1 786	5 747	1 522	7 714	1 996	6 172	1 607
0.8	7 321	1 834	5 864	1 597	7 973	2 066	6 290	1 673
1.0	7 509	1 888	5 933	1 654	8 211	2 127	6 443	1 741

Table 6. Variation of t_p (*10^{-6} in seconds) with different α_1 and constant $\frac{a}{b} = 1.5$ for all X and Y, see Figure 6.

modes. The graph shown in Figure 5 shows that the period (t_p) decreases as β_2 increases for both modes of vibration.

Table 6 deals with the variation of t_p (*10^{-6} in seconds) with different α_1(0.0, 0.2, 0.4, 0.6, 0.8, 1.0) and constant $\frac{a}{b} = 1.5$ for all X and Y. It is observed that the value of t_p increases as α_1 increases from 0.0 to 1.0 for both modes of vibration. The results shown in Table 6 are supported by the graph shown in Figure 6.

Tables 7–9 show the value of w (*10^{-5}) for the constant $\frac{a}{b} = 1.5$ and for different X and Y with three different variations of the values of α, β_1, β_2 and α_1 given by ($\alpha = \beta_1 = \beta_2 = \alpha_1 = 0.0$), ($\alpha = \beta_1 = \beta_2 = 0.0$, $\alpha_1 = 0.4$), ($\alpha = 0.2$, $\beta_1 = 0.3$, $\beta_2 = 0.4$, $\alpha_1 = 0.4$), respectively. From these tables, it can clearly be seen that as $\bar{X}$ increases for different values of $\bar{Y}$, the value of w first increases and then decreases to zero for the first mode of vibration. For the second mode of vibration, it can be seen that the

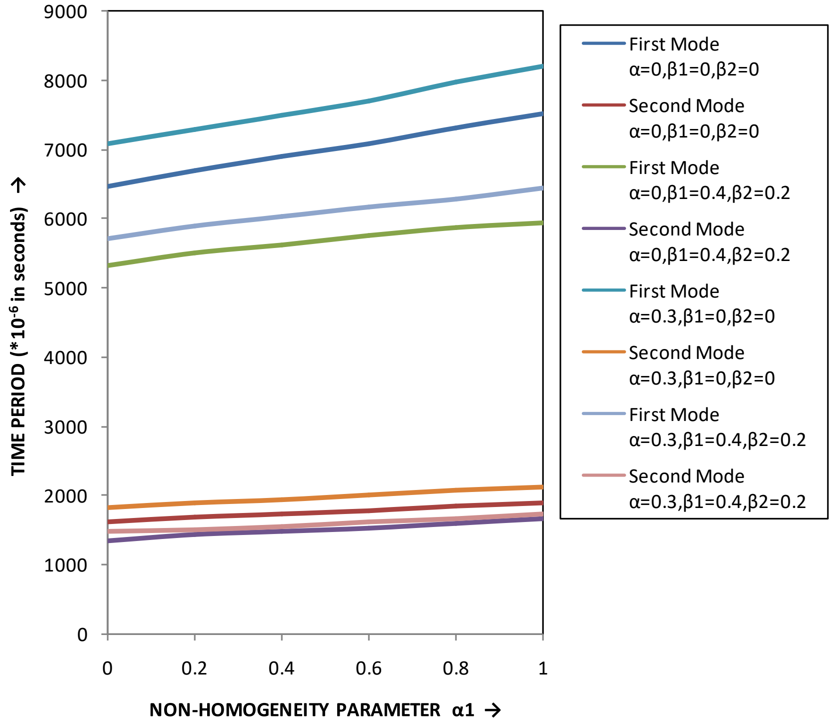

FIGURE 6. Variation of t_p (*10^{-6} in seconds) with different α_1 and constant $\frac{a}{b} = 1.5$ for all X and Y.

	Mode → $\bar{X}$ ↓	$Y = 0.20$ I	$Y = 0.20$ II	$Y = 0.60$ I	$Y = 0.60$ II
Time $= 0.0 \times t_p$	0.0	0.0	0.0	0.0	0.0
	0.2	126.32	38.87	427.32	14.52
	0.4	303.71	6.12	1420.12	26.73
	0.6	303.71	6.12	1420.12	26.73
	0.8	126.32	38.87	427.32	14.52
	1.0	0.0	0.0	0.0	0.0
Time $= 5.0 \times t_p$	0.0	0.0	0.0	0.0	0.0
	0.2	55.12	1.38	187.31	0.53
	0.4	132.32	0.21	623.16	1.01
	0.6	132.32	0.21	623.16	1.01
	0.8	55.12	1.38	187.31	0.53
	1.0	0.0	0.0	0.0	0.0

TABLE 7. w(*10^{-5}) for constant $\frac{a}{b} = 1.5$ and $\alpha = \beta_1 = \beta_2 = \alpha_1 = 0.0$ and for different X and Y, see Figure 7.

value of w for $Y = 0.2$, the value changes frequently as it first increases and then decreases, then repeats this trend by increasing again and finally becoming zero as $\bar{X}$ increases but for $Y = 0.6$, with the increase in X, the value of w varies as it first increases and then it decreases until it reaches zero. The graphs in Figures 7, 8 and 9 support the results of Tables 7–9.

Tables 10–12 represent the deflection w (*10^{-5}) for $X = Y = 0.2$ and for three different cases, namely (for different $\frac{a}{b}$ and $\alpha = \beta_1 = \beta_2 = \alpha_1 = 0.0$), (for different $\frac{a}{b}$ and $\alpha = \beta_1 = \beta_2 = 0.0$, $\alpha_1 = 0.4$) and (for different $\frac{a}{b}$ and $\alpha = 0.3$, $\beta_1 = 0.3$, $\beta_2 = 0.4$, $\alpha_1 = 0.4$) respectively. From these tables, it can be seen that the value of w increases continuously at time $0.0 \times t_p$, it is also observed that with the increase there is slight decrease at the time $5.0 \times t_p$ for the first mode of vibration but it is also noticed that the decrease follows the increase in the value of $\frac{a}{b}$ from 0.5 to 2.5, at time $0.0 \times t_p$ and at time $5.0 \times t_p$ for the second mode of vibration. These results are also supported by the graphs shown in Figures 10–12.

6. COMPARISON OF THE RESULTS OF THE PRESENT STUDY WITH THE PREVIOUS STUDY

The time function and the deflection results obtained in the present study are compared with those of the reference [13]. The comparison of the results of these

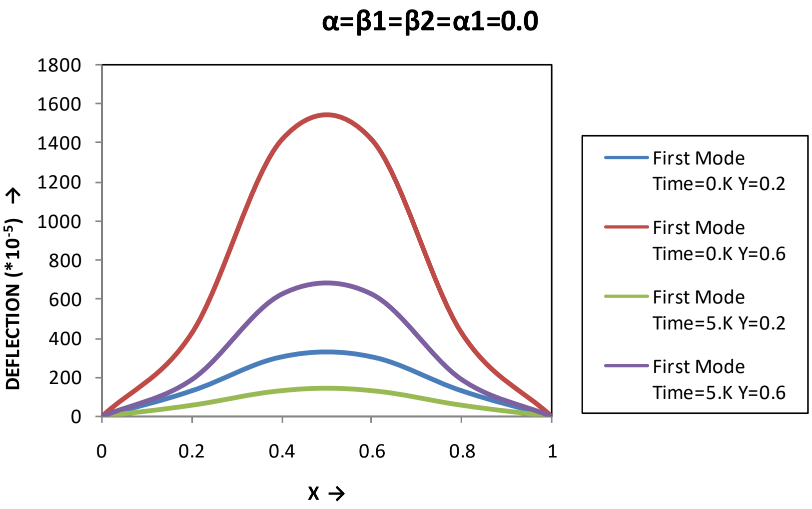

(a). First mode.

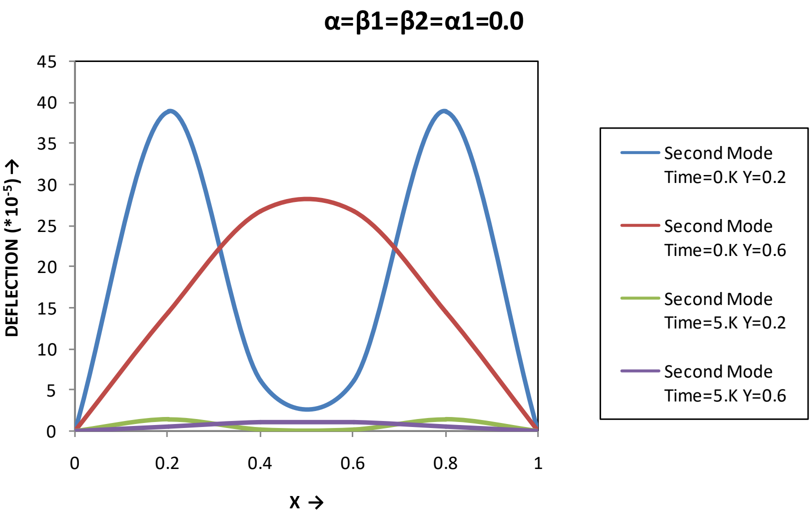

(b). Second mode.

Figure 7. Variation of $w(*10^{-5})$ with different X for constant $\frac{a}{b} = 1.5$ and $\alpha = \beta_1 = \beta_2 = \alpha_1 = 0.0$ and for different Y.

	Mode → $\bar{X}$ ↓	$Y = 0.20$ I	$Y = 0.20$ II	$Y = 0.60$ I	$Y = 0.60$ II
Time $= 0.0 \times t_p$	0.0	0.0	0.0	0.0	0.0
	0.2	130.43	40.12	431.01	15.93
	0.4	307.69	6.96	1 424.07	28.12
	0.6	307.69	6.96	1 424.07	28.12
	0.8	130.43	40.12	431.01	15.93
	1.0	0.0	0.0	0.0	0.0
Time $= 5.0 \times t_p$	0.0	0.0	0.0	0.0	0.0
	0.2	59.13	1.93	190.34	0.83
	0.4	136.32	0.43	627.65	1.17
	0.6	136.32	0.43	627.65	1.17
	0.8	59.13	1.93	190.34	0.83
	1.0	0.0	0.0	0.0	0.0

Table 8. $w(*10^{-5})$ for constant $\frac{a}{b} = 1.5$ and $\alpha = \beta_1 = \beta_2 = 0.0$, $\alpha_1 = 0.4$ and for different X and Y, see Figure 8.

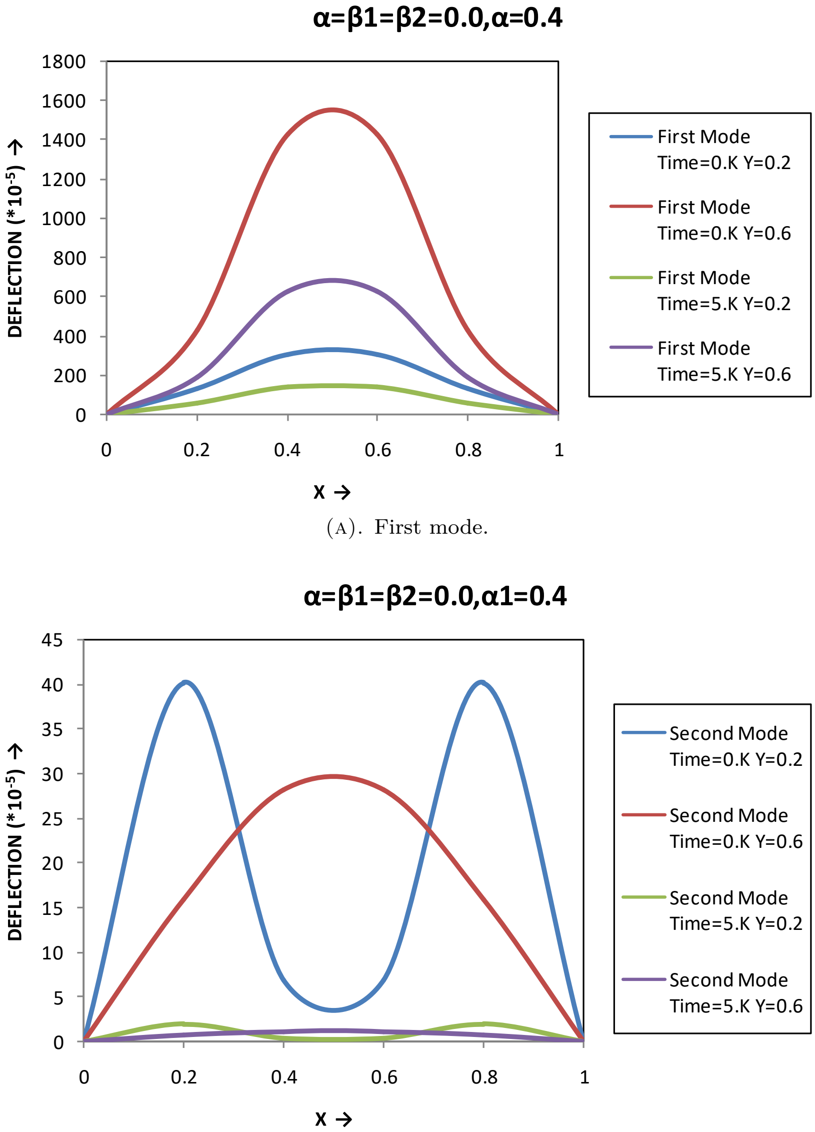

(a). First mode.

(b). Second mode.

Figure 8. Variation of $w(*10^{-5})$ with different X for constant $\frac{a}{b} = 1.5$ and $\alpha = \beta_1 = \beta_2 = 0.0$, $\alpha_1 = 0.4$ and for different Y.

	Mode → $\bar{X}$ ↓	$Y = 0.20$ I	$Y = 0.20$ II	$Y = 0.60$ I	$Y = 0.60$ II
Time $= 0.0 \times t_p$	0.0	0.0	0.0	0.0	0.0
	0.2	233.72	40.12	3 196.18	15.22
	0.4	654.68	6.94	10 753.11	27.83
	0.6	654.68	6.94	10 753.11	27.83
	0.8	233.72	40.12	3 196.18	15.22
	1.0	0.0	0.0	0.0	0.0
Time $= 5.0 \times t_p$	0.0	0.0	0.0	0.0	0.0
	0.2	96.12	1.13	1 290.07	0.47
	0.4	258.24	0.21	4 209.84	0.69
	0.6	258.24	0.21	4 209.84	0.69
	0.8	96.12	1.13	1 290.07	0.47
	1.0	0.0	0.0	0.0	0.0

Table 9. $w(*10^{-5})$ for constant $\frac{a}{b} = 1.5$ and $\alpha = 0.2$, $\beta_1 = 0.3$, $\beta_2 = \alpha_1 = 0.4$ and for different X and Y, see Figure 9.

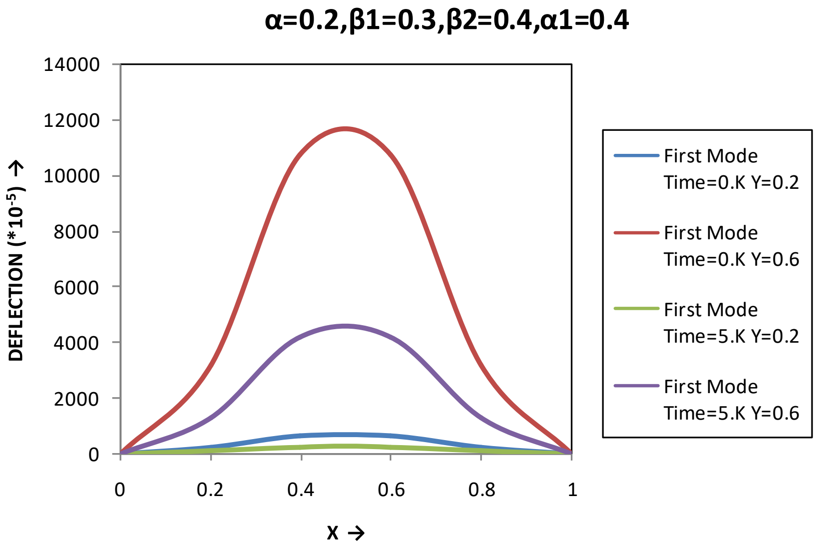

(A). First mode.

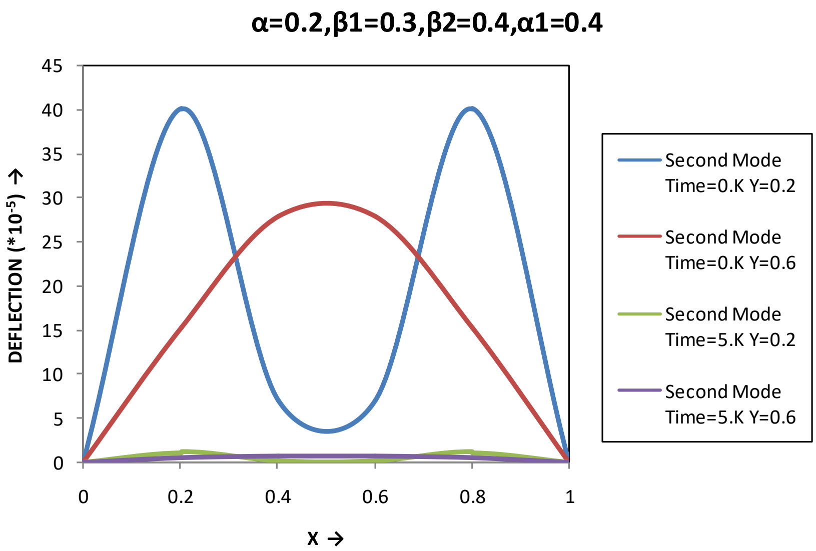

(B). Second mode.

FIGURE 9. Variation of $w(*10^{-5})$ with different X for constant $\frac{a}{b} = 1.5$ and $\alpha = 0.2$, $\beta_1 = 0.3$, $\beta_2 = \alpha_1 = 0.4$ and for different Y.

Mode → $\frac{a}{b}$ ↓	Time $= 0.0 \times t_p$ I	II	Time $= 5.0 \times t_p$ I	II
0.5	20.93	14.02	14.34	3.63
1.0	63.12	32.41	38.67	4.84
1.5	126.32	38.87	55.12	1.38
2.0	233.96	37.37	61.42	0.14
2.5	398.28	36.09	53.21	0.003

TABLE 10. $w(*10^{-5})$ for different $\frac{a}{b}$ and $\alpha = \beta_1 = \beta_2 = \alpha_1 = 0.0$ and for $X = Y = 0.2$, see Figure 10.

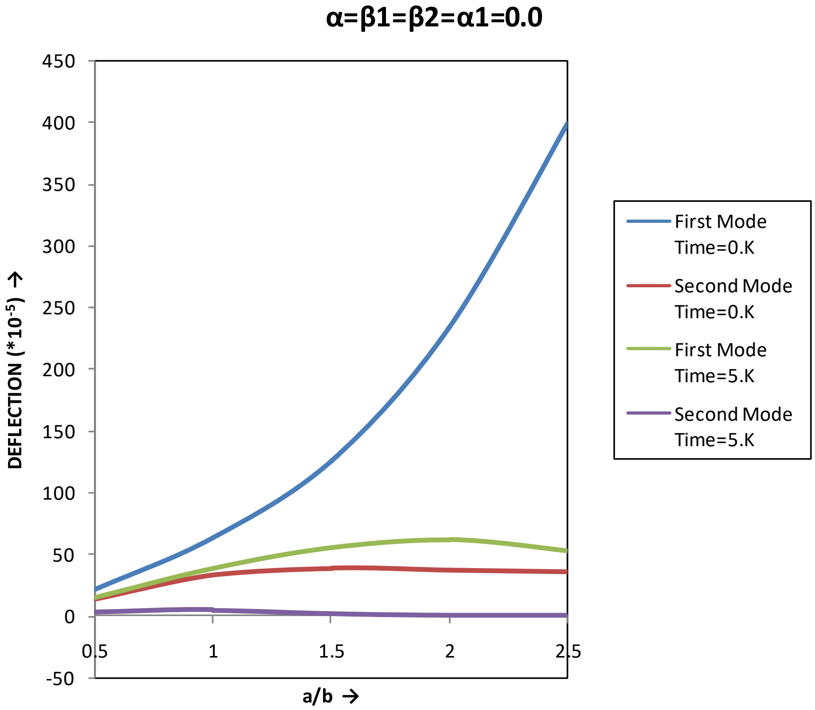

FIGURE 10. Variation of $w(*10^{-5})$ for different $\frac{a}{b}$ and $\alpha = \beta_1 = \beta_2 = \alpha_1 = 0.0$ and for $X = Y = 0.2$.

Mode → $\frac{a}{b}$ ↓	Time $= 0.0 \times t_p$ I	Time $= 0.0 \times t_p$ II	Time $= 5.0 \times t_p$ I	Time $= 5.0 \times t_p$ II
0.5	24.23	15.33	17.68	4.37
1.0	66.84	33.97	41.32	5.60
1.5	130.43	40.12	59.13	1.93
2.0	238.27	39.11	64.92	0.21
2.5	403.03	37.28	57.16	0.006

TABLE 11. $w(*10^{-5})$ for different $\frac{a}{b}$ and $\alpha = \beta_1 = \beta_2 = 0.0$, $\alpha_1 = 0.4$ and for $X = Y = 0.2$, see Figure 11.

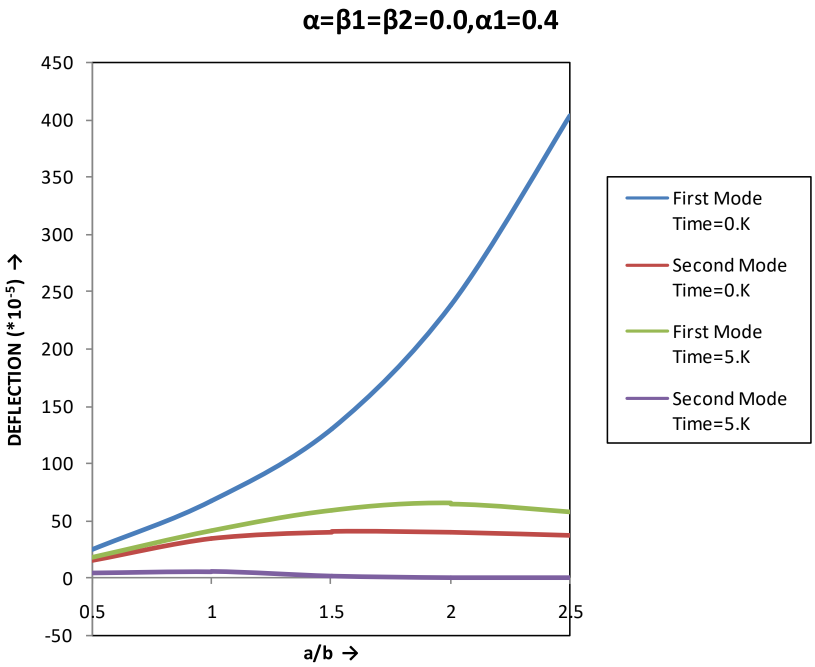

FIGURE 11. Variation of $w(*10^{-5})$ for different $\frac{a}{b}$ and $\alpha = \beta_1 = \beta_2 = 0.0$, $\alpha_1 = 0.4$ and for $X = Y = 0.2$.

Mode → $\frac{a}{b}$ ↓	Time = $0.0 \times t_p$ I	II	Time = $5.0 \times t_p$ I	II
0.5	28.03	15.73	21.53	3.64
1.0	96.67	33.78	58.45	4.34
1.5	235.72	40.31	98.27	1.29
2.0	501.18	38.92	121.02	0.099
2.5	935.23	37.35	109.33	0.00053

Table 12. $w(*10^{-5})$ for different $\frac{a}{b}$ and $\alpha = \beta_1 = 0.3$, $\beta_2 = \alpha_1 = 0.4$ and for $X = Y = 0.2$, see Figure 12.

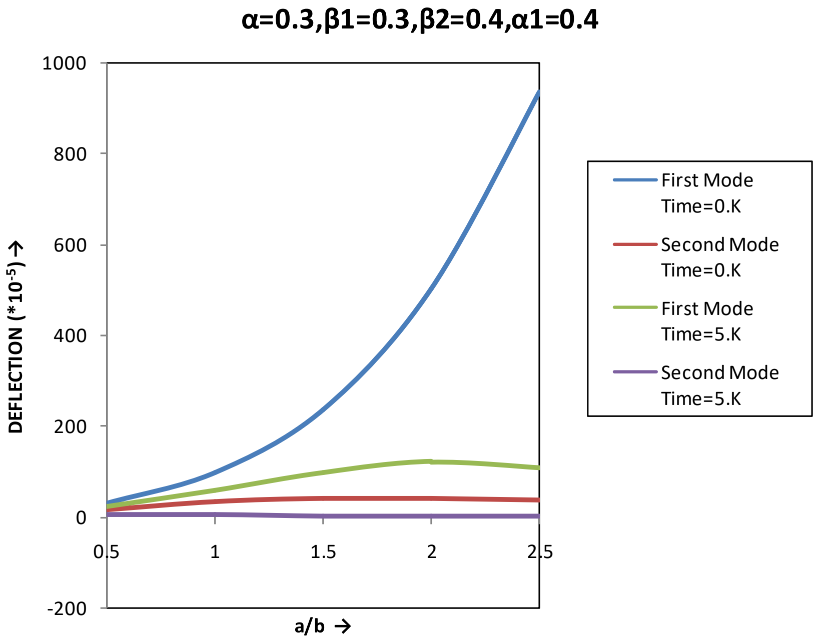

Figure 12. Variation of $w(*10^{-5})$ for different $\frac{a}{b}$ and $\alpha = \beta_1 = 0.3$, $\beta_2 = \alpha_1 = 0.4$ and for $X = Y = 0.2$.

	$\alpha_1 = 0.0$, $\alpha = 0.0$, $\frac{a}{b} = 1.5$				$\alpha_1 = 0.4$, $\alpha = 0.0$, $\frac{a}{b} = 1.5$			
	$\beta_1 = 0.0$		$\beta_1 = 0.4$		$\beta_1 = 0.0$		$\beta_1 = 0.4$	
	$\beta_2 = 0.0$		$\beta_2 = 0.2$		$\beta_2 = 0.0$		$\beta_2 = 0.2$	
Mode →	I	II	I	II	I	II	I	II
Present Study	6 462	1 623	5 324	1 332	6 897	1 728	5 543	1 433
[13]	6 462	1 623	5 324	1 332	6 883	1 724	5 531	1 428

Table 13. The comparative data of the time period with the reference [13].

	$\alpha_1 = \alpha = \beta_1 = \beta_2 = 0.0$				$\alpha_1 = 0.4$, $\alpha = \beta_1 = \beta_2 = 0.0$			
	$\frac{a}{b} = 1.0$		$\frac{a}{b} = 2.0$		$\frac{a}{b} = 1.0$		$\frac{a}{b} = 2.0$	
Mode →	I	II	I	II	I	II	I	II
Present Study	10 411	2 638	3 724	905	10 860	2 747	4 082	961
[13]	10 411	2 638	3 724	905	10 847	2 741	4 073	958

Table 14. The comparative data of the time period with the reference [13].

two studies for the time function is shown in Tables 13–15 while the comparison of the results of the deflection are shown in Tables 16–21. The Tables 13–15 show that the results of the period for the present study and the reference [13] are identical when the value of the constant of non-homogeneity (α_1) is zero. These tables also show that the quadratic variation in the material density of the plate along the x-axis is more dominant as compared to that along the x-axis. Tables 16–18 show that the results of the deflection for the present study and the reference [13] are identical when the value of the constant of non-homogeneity (α_1) is zero. The results shown in Tables 19–21 indicate that the quadratic variation in the material density of the

	$\alpha_1 = 0.0,\ \alpha = 0.6,\ \frac{a}{b} = 1.5$				$\alpha_1 = 0.4,\ \alpha = 0.6,\ \frac{a}{b} = 1.5$			
	$\beta_1 = 0.0$		$\beta_1 = 0.4$		$\beta_1 = 0.0$		$\beta_1 = 0.4$	
	$\beta_2 = 0.0$		$\beta_2 = 0.2$		$\beta_2 = 0.0$		$\beta_2 = 0.2$	
Mode →	**I**	**II**	**I**	**II**	**I**	**II**	**I**	**II**
Present Study	7 737	2 002	6 213	1 603	8 497	2 176	6 626	1 759
[13]	7 737	2 002	6 213	1 603	8 486	2 173	6 617	1 756

TABLE 15. The comparative data of the time period with the reference [13].

	Time = 0.0 × t_p		**Time = 5.0 × t_p**	
Mode →	**I**	**II**	**I**	**II**
Present Study	126.32	38.87	55.12	1.38
[13]	126.32	38.87	55.12	1.38

TABLE 16. The comparative data of the deflection with the reference [13]; $\alpha = \beta_1 = \beta_2 = \alpha_1 = 0.0$, $\frac{a}{b} = 1.5$, $X = Y = 0.20$.

	Time = 0.0 × t_p		**Time = 5.0 × t_p**	
Mode →	**I**	**II**	**I**	**II**
Present Study	233.96	37.37	61.42	0.14
[13]	233.96	37.37	61.42	0.14

TABLE 17. The comparative data of the deflection with the reference [13]; $\alpha = \beta_1 = \beta_2 = \alpha_1 = 0.0$, $\frac{a}{b} = 2.0$, $X = Y = 0.20$.

	Time = 0.0 × t_p		**Time = 5.0 × t_p**	
Mode →	**I**	**II**	**I**	**II**
Present Study	427.32	14.52	187.31	0.53
[13]	427.32	14.52	187.31	0.53

TABLE 18. The comparative data of the deflection with the reference [13]; $\alpha = \beta_1 = \beta_2 = \alpha_1 = 0.0$, $\frac{a}{b} = 1.5$, $X = 0.20$, $Y = 0.60$.

	Time = 0.0 × t_p		**Time = 5.0 × t_p**	
Mode →	**I**	**II**	**I**	**II**
Present Study	130.43	40.12	59.13	1.93
[13]	128.62	39.74	57.36	1.58

TABLE 19. The comparative data of the deflection with the reference [13]; $\alpha = \beta_1 = \beta_2 = \alpha_1 = 0.4$, $\frac{a}{b} = 1.5$, $X = Y = 0.20$.

	Time = 0.0 × t_p		**Time = 5.0 × t_p**	
Mode →	**I**	**II**	**I**	**II**
Present Study	238.27	39.11	64.92	0.21
[13]	236.43	38.15	63.88	0.18

TABLE 20. The comparative data of the deflection with the reference [13]; $\alpha = \beta_1 = \beta_2 = \alpha_1 = 0.4$, $\frac{a}{b} = 2.0$, $X = Y = 0.20$.

	Time = 0.0 × t_p		**Time = 5.0 × t_p**	
Mode →	**I**	**II**	**I**	**II**
Present Study	431.01	15.93	190.34	0.83
[13]	428.52	15.02	188.82	0.64

TABLE 21. The comparative data of the deflection with the reference [13]; $\alpha = \beta_1 = \beta_2 = \alpha_1 = 0.4$, $\frac{a}{b} = 1.5$, $X = 0.20$, $Y = 0.60$.

plate along the x-axis is more dominant as compared to that along the x-axis. The comparative study of the present results with the reference [13] using Tables 13–21 ensure the accuracy and the validity of the derived formulas and the results of this study.

7. Conclusion

The author effectively discussed the non-homogeneity effect on the vibration of the rectangular visco-elastic plate subjected to the linear temperature effect with both the directions quadratic thickness variation. The results show that as the non-homogeneity constant increases for both modes of vibration, the time function and the deflection continuously increase (frequency decreases), therefore the effect of non-homogeneity on vibrations cannot be neglected. The results of this paper also show that the effect of taper is more dominant in the x-direction as compared to that of the y-direction.

References

[1] A. W. Leissa. *NASA SP-160. Vibration of plates.* U.S. Government Printing Office, Washington, D.C., USA, 1969.

[2] G. S. Sharma, A. Sarkar. Directivity-based passive barrier for local control of low-frequency noise. *Journal of Theoretical and Computational Acoustics* **26**(4):1850012, 2018. https://doi.org/10.1142/S2591728518500123

[3] G. S. Sharma, A. Sarkar. Directivity based control of acoustic radiation. *Applied Acoustics* **154**:226–235, 2019. https://doi.org/10.1016/j.apacoust.2019.04.031

[4] A. K. Gupta, L. Kumar. Thermal effect on vibration of non-homogenous visco-elastic rectangular plate of linearly varying thickness. *Meccanica* **43**(1):47–54, 2008. https://doi.org/10.1007/s11012-007-9093-3

[5] A. K. Gupta, A. Khanna. Vibration of visco-elastic rectangular plate with linearly thickness variations in both directions. *Journal of Sound and Vibration* **301**(3–5):450–457, 2007. https://doi.org/10.1016/j.jsv.2006.01.074

[6] P. A. A. Laura, R. H. Gutierrez. Comments on "Vibration analysis of a rectangular plate subjected to a thermal gradient". *Journal of Sound and Vibration* **72**(2):263, 1980. https://doi.org/10.1016/0022-460X(80)90656-2

[7] A. K. Gupta, T. Johri, R. P. Vats. Study of thermal gradient effect on vibrations of a non-homogeneous orthotropic rectangular plate having bi-direction linearly thickness variations. *Meccanica* **45**(3):393–400, 2010. https://doi.org/10.1007/s11012-009-9258-3

[8] A. K. Gupta, H. Kaur. Study of the effect of thermal gradient on free vibration of clamped visco-elastic rectangular plates with linearly thickness variation in both directions. *Meccanica* **43**(4):449–458, 2008. https://doi.org/10.1007/s11012-008-9110-1

[9] B. Singh, V. Saxena. Transverse vibration of a rectangular plate with bidirectional thickness variation. *Journal of Sound and Vibration* **198**(1):51–65, 1996. https://doi.org/10.1006/jsvi.1996.0556

[10] M. S. Dhotarad, N. Ganesan. Vibration analysis of a rectangular plate subjected to a thermal gradient. *Journal of Sound and Vibration* **60**(4):481–497, 1978. https://doi.org/10.1016/S0022-460X(78)80087-X

[11] A. K. Gupta, A. Khanna, S. Kumar, et al. Vibration analysis of visco-elastic rectangular plate with thickness varies linearly in one and parabolically in other direction. *Advanced Studies in Theoretical Physics* **4**(15):743–758, 2010.

[12] A. K. Gupta, S. Aggarwal. Vibration of non-homogeneous visco-elastic rectangular plate having linearly varying thickness in both directions with thermal gradient effect. *Journal of Advanced Research in Applied Mathematics and Statistics* **3**(1–2):19–28, 2018.

[13] A. K. Gupta, S. Aggarwal. Non-homogeneous effect on vibration of visco-elastic rectangular plate having parabolically varying thickness in both directions. *Journal of Experimental & Applied Mechanics* **9**(3):1–17, 2018.

[14] A. K. Gupta, S. Aggarwal. Thermally induced vibration of non-homogeneous visco-elastic rectangular plate of variable thickness. *International Journal of Research in Advent Technology* **6**(5):768–777, 2018.

[15] A. K. Gupta, H. Kaur. Effect of thermal gradient on vibration of clamped visco-elastic rectangular plate with exponentially thickness variation in both the directions. *American Journal of Computational and Applied Mathematics* **3**(1):36–45, 2013. https://doi.org/10.5923/j.ajcam.20130301.07

[16] K. Nagaya. Vibrations and dynamic response of viscoelastic plates on nonperiodic elastic supports. *Journal of Manufacturing Science and Engineering* **99**(2):404–409, 1977. https://doi.org/10.1115/1.3439251

[17] A. K. Gupta, H. Kaur, S. Kumar. Thermal effect on vibration of clamped visco-elastic rectangular plate with parabolic thickness variation in both directions. *Shock and Vibration* **17**:93–105, 2010. https://doi.org/10.3233/SAV-2010-0500

[18] R. B. Bhat. Natural frequencies of rectangular plates using characteristic orthogonal polynomials in Rayleigh-Ritz method. *Journal of Sound and Vibration* **102**(4):493–499, 1985. https://doi.org/10.1016/S0022-460X(85)80109-7

[19] J. S. Tomar, A. K. Gupta. Thermal effect on frequencies of an orthotropic rectangular plate of linearly varying thickness. *Journal of Sound and Vibration* **90**(3):325–331, 1983. https://doi.org/10.1016/0022-460X(83)90715-0

[20] R. Saini, R. Lal. Transverse vibration of non-homogeneous rectangular plates of variable thickness using GDQ. *International Journal of Engineering, Mathematical and Physical Sciences* **8**(9):1211–1216, 2014.

[21] A. K. Gupta, M. Saini, S. Singh, R. Kumar. Forced vibrations of non-homogeneous rectangular plate of linearly varying thickness. *Journal of Vibration and Control* **20**(6):876–884, 2014. https://doi.org/10.1177/1077546312466883

[22] M. G. Sobamowo, S. A. Salawu, A. A. Yinusa, O. D. Makinde. Nonlinear thermally induced dynamic analysis of non-homogenous rectangular plate with varying thickness using three-dimensional differential transform method. *World Scientific News* **138**(2):141–166, 2019.

[23] A. K. Gupta, J. Mamta. Exponential temperature effect on frequencies of a rectangular plate of non-linear varying thickness: A quintic spline technique. *Journal of Theoretical and Applied Mechanics* **52**(1):15–24, 2014.

[24] P. Singhal, Ruby. A scientific approach on thermally induced vibrations of non-homogeneous tapered rectangular plate. *A Journal of Composition Theory* **12**(7):875–882, 2023.

[25] Y.-L. Yeh, M.-J. Jang, C. C. Wang. Analyzing the free vibrations of a plate using finite difference and differential transformation method. *Applied Mathematics and Computation* **178**(2):493–501, 2006. https://doi.org/10.1016/j.amc.2005.11.068

[26] A. Khanna, A. Singhal. Influence of temperature variation on vibration of rectangular plate of visco-elastic material. *World Scientific News* **139**(2):61–75, 2020.

[27] N. Jafari, M. Azhari. Free vibration analysis of viscoelastic plates with simultaneous calculation of natural frequency and viscous damping. *Mathematics and Computers in Simulation* **185**:646–659, 2021. https://doi.org/10.1016/j.matcom.2021.01.019

[28] M. Amabili, P. Balasubramanian, G. Ferrari. Nonlinear vibrations and damping of fractional viscoelastic rectangular plates. *Nonlinear Dynamics* **103**(4):3581–3609, 2021. https://doi.org/10.1007/s11071-020-05892-0

[29] R. Bhardwaj, N. Mani, A. Sharma. Time period of transverse vibration of skew plate with parabolic temperature variation. *Journal of Vibration and Control* **27**(3–4):323–331, 2021. https://doi.org/10.1177/1077546320926887

[30] R. Abdikarimov, M. Amabili, N. I. Vatin, D. Khodzhaev. Dynamic stability of orthotropic viscoelastic rectangular plate of an arbitrarily varying thickness. *Applied Sciences* **11**(13):6029, 2021. https://doi.org/10.3390/app11136029